The skull roof tracks the brain during the evolution and development of reptiles including birds

Matteo Fabbri[1]*, Nicolás Mongiardino Koch[1], Adam C. Pritchard[1], Michael Hanson[1], Eva Hoffman[1,5], Gabriel S. Bever[2], Amy M. Balanoff[2], Zachary S. Morris[3], Daniel J. Field[1,4], Jasmin Camacho[3], Timothy B. Rowe[5], Mark A. Norell[6], Roger M. Smith[7], Arhat Abzhanov[8,9]*, Bhart-Anjan S. Bhullar[1]*

1 Department of Geology and Geophysics and Peabody Museum of Natural History, Yale University, New Haven, CT 06520, USA

2 Center for Functional Anatomy and Evolution, Johns Hopkins University School of Medicine, Baltimore, MD 21205, USA

3 Department of Organismal and Evolutionary Biology and Museum of Comparative Zoology, Harvard University, Cambridge, MA 02138, USA

4 Milner Centre for Evolution, Department of Biology and Biochemistry, University of Bath, Bath, BA2 7AY, UK

5 Current address: Jackson School of Geosciences and Vertebrate Paleontology Laboratory, The University of Texas at Austin, Austin, TX 78705, USA

6 Macaulay Curator, Division of Paleontology, American Museum of Natural History, New York, NY 10024, USA

7 Natural History Department, Iziko South African Museum, Cape Town 8000, South Africa

8 Department of Life Sciences, Imperial College London, Silwood Park Campus, Ascot, Berkshire SL5 7PY, United Kingdom

9 Natural History Museum, London SW7 5BD, United Kingdom

*Corresponding authors

Emails: matteo.fabbri@yale.edu; a.abzhanov@nhm.ac.uk; bhart-anjan.bhullar@yale.edu.

Major transformations in brain size and proportions, such as the enlargement of the brain during the evolution of birds, are accompanied by profound modifications to the skull roof. However, the hypothesis of concerted evolution of shape between brain and skull roof over major phylogenetic transitions, and in particular of an ontogenetic relationship between specific regions of the brain and the skull roof, has never been formally tested. We performed 3D

morphometric analyses to examine the deep history of brain and skull-roof morphology in Reptilia, focusing on changes during the well-documented transition from early reptiles through archosauromorphs including nonavian dinosaurs to birds. Non-avialan taxa cluster tightly together in morphospace, whereas *Archaeopteryx* and crown birds occupy a separate region. There is a one-to-one correspondence between the forebrain and frontal and the midbrain and parietal. Furthermore, the position of the forebrain–midbrain boundary correlates significantly with the position of the frontoparietal suture in across the phylogenetic breadth of Reptilia and during the ontogeny of individual taxa. Conservation of position and identity in the skull roof is apparent, and there is no support for prior hypotheses that the avian parietal is a transformed postparietal. The correlation and apparent developmental link between regions of the brain and bony skull elements are likely ancestral to Tetrapoda and may be fundamental to all of Osteichthyes, coeval with the origin of the dermatocranium.

Introduction

The brain is often considered to have a peculiar primacy in the development of the head[e.g.1-4]. A general developmental relationship between brain and skull, with an emphasis on the facial region, has been well documented across tetrapods[1-12] – however, associations between particular regions of the brain and the primordia of individual elements of the skull roof have not been shown, despite the fact that these associations speak to both the patterning and the identity of the bones of the head. The skull roof or cranial vault directly overlies the brain; its largest constituents are the frontal bone anteriorly, between the orbits, and the parietal bone posteriorly, between the adductor muscle chambers. The homologies of these bones are a subject of recent contention based on developmental evidence, especially along the transition from small-brained nonavian reptile ancestors to large-brained birds (Aves)[13-15]. Early studies concluded that the entire frontal in chicken was developmentally derived from cells of the neural crest[e.g. 16], as is the case in mouse and axolotl[5-6,17], whereas later works suggested a composite germ-layer origin, with cranial neural crest contributing to the anterior part of the frontal and mesoderm to the posterior[17-18]. The latter interpretation inspired a hypothesis that the avian frontal actually represents a fusion of the frontal and parietal

bones of other reptiles, and that the avian parietal is in fact the postparietal or interparietal, an ossification or pair of ossifications seen in primitive Amniota[18]. This brings into question the identity, homology (defined as homology=synapomorphy for this study, or secondary homology *sensu* De Pinna[19]), and nomenclature of the skull elements in Aves relative to its successive sister taxa. We qualitatively and quantitatively examined the relationship of the brain to the skull roof from a combined phylogenetic and ontogenetic perspective. We wished in particular to trace the evolution of brain and skull roof through the entire history of Archosauromorpha and to resolve the conundrum concerning the identity and homology of skull-roof elements in crown birds. Contrary to previous studies[17], we found no support for a fused origin of the avian frontal and a resulting shift in skull-roof element identity in birds. Our data instead suggest that the dominant developmental influence on the identity of individual skull-roof elements is the organization of the brain at its three-vesicle stage, and that a strict correlation between regions of the brain and particular skull-roof elements, specifically between the forebrain (derived from the embryonic prosencephalon) and the frontal and the midbrain (derived from the embryonic mesencephalon) and the parietal, is present at least across all amniotes. Morphological correlation of course is not sufficient to demonstrate developmental mechanism, and we hope that our findings inspire evolutionarily informed searches for the molecular patterning responsible for correspondences between early embryonic structures and the later-appearing ossified skeleton.

To test the hypothesis that there is a close relationship between brain and skull roof, we used 3D geometric morphometrics and comparative embryology to explore the association between these structures along the entire stem and crown reptile lineage, including Lepidosauria (lizards, snakes, and tuataras), Crocodylia, and Avialae, as well as stem-group Crocodylia, stem-group Archosauria, and stem-group reptiles (Fig. 1a). This sample includes pivotal taxa whose endocranial spaces and surrounding bones have never been examined (see Table S1 for a list of taxa included in this study)[20-21]. Extant taxa included embryonic series for alligator (*Alligator mississippiensis*) and chicken (*Gallus gallus*), which were stained to reveal soft tissues. When embryonic skull roofs were not sufficiently ossified, we used contrast-stained brains to extract brain shapes directly (see supplemental material for general methods used and protocols in staining).

Results and Discussion

Our data revealed an overall conservation of skull-roof architecture across Reptilia, as well as conservation in the relationship between the skull roof and the brain. The adult frontal always lies over the forebrain, whereas the adult parietal lies either over the midbrain or over a combination of midbrain and posterior forebrain (Fig. 1b-d, Fig. 2). The postparietal, when present in extinct reptiles, is a diminutive dermal element that does not directly overlie the brain. It is generally excluded from contacting the *dura mater* by the parietals and supraoccipital (Fig. 1b, Fig. 2). Its most consistent relationship is with the nuchal musculature, which can be reconstructed to have attached broadly to its posterior surface (Fig. 1b).

The postparietal is lost in Lepidosauria[22] (Fig. 1a, Fig. 2). It is commonly present, with some exceptions, along the archosaurian stem, and then almost completely disappears prior to the divergence of Archosauria[23]. We confirmed, however, one case of reappearance of the postparietal within the crocodile lineage: our CT scans of *Gracilisuchus stipanicorum* show clear sutures between the parietals and the element posited to be a secondarily acquired postparietal[24] (Fig. 1a-b, Fig. 2). Previous work has questioned the identity of the element and its distinction from the parietal[23]. The reacquired postparietal of *G. stipanicorum* is small and, as expected, does not border the endocranial space. In all the postparietals present in the extinct reptiles we examined, we could find neither anatomical nor topological points of similarity that could be used to suggest primary homology with dinosaurian, including avian, parietals, though it is possible that in some cases the small postparietal was absorbed by the parietals to form a minute posterior eminence.

Despite an overall conservation of organization in the reptile cranium, we also detected major evolutionary alterations to its architecture. Three-dimensional morphometric comparative analyses (Fig. 3, Fig. S1-S2, Table S1 and list of landmarks used in SI) yield a tight cluster that comprises non-avialan dinosaurs, crocodile-line (pseudosuchian) archosaurs, stem archosaurs, lepidosaurs, and stem reptiles. This clustering arises despite an evolutionary divergence of 250 million years, an extremely wide range of apparent ecological niches, and a size range of several orders of magnitude, from small *Anolis* lizards (Squamata) to giant tyrannosaurs. PC 1 captures the transverse expansion of the brain and skull roof as well as the posterior shift of the forebrain–midbrain

boundary and the frontoparietal suture, while PC 2 represents the reduction of the parietal relative to the frontal, the expansion of the frontal, and the relative inflation of the forebrain and the cerebellum (Fig. S3). The presence or absence of a postparietal does not seem to influence the clustering of taxa in morphospace. One of the most divergent clusters is composed of the giant allosauroids *Allosaurus* and *Acrocanthosaurus*. Their aberrant position appears to be driven solely by the depth of the skull roof, possibly for the attachment of jaw muscles, as the deepening drastically increases the surface area of lateral adductor attachment sites on the parietal[20,23]. Brain endocasts of the giant allosauroids fall out with those of the other conservative taxa (Fig. 3c, Fig. S2). *Archaeopteryx* and crown birds diverge from the more conservative cluster along PC 1 (Fig. 3-S2); *Archaeopteryx* is closer to crown birds than to non-avialan maniraptorans in brain and skull-roof shape despite having a plesiomorphic endocranial volume[2].

The inclusion of ontogenetic series for chicken and alligator revealed that, relative to alligator ontogeny, chicken ontogeny is morphologically short. Brains and skull roofs of chicken embryos are similar to those of adults, despite a sample that extends from early embryos to large adults. The ontogenetic trajectory of alligator is longer, traversing a distance in morphospace equivalent to 134% that of chicken. Alligator embryos clustered with crown birds and *Archaeopteryx* in the combined and skull-roof analyses, whereas they fell within the cluster of more conservative taxa when we included only the brain (Fig. 3b-c). We noted a negative allometry between the brain and skull during the development of alligators: the brain is relatively large in the early stages of development and becomes smaller with respect to the skull during growth. On the other hand, birds have a very large brain at hatching relative to the skull, and the brain continues to expand during ontogeny, growing with positive allometry. We suggest that the brain in Aves should be considered peramorphic in recognition of earlier onset of growth, faster sustained growth, and absolutely larger adult size in comparison with all but the most crownward non-avian avialans.

Given the generally consistent clustering of taxa on the brain and skull-roof morphometric plots, we expected to find a correspondence between regions of the brain and bony elements of the skull roof. First, we tested and failed to reject the hypothesis of integration (similar levels of covariation for morphological traits between and within modules) between the skull roof and brain across the

142 evolutionary history of reptiles (CR = 0.982, P = 0. 092), a finding contrary to previous studies[e.g.
143 3]. This result reveals that, despite major morphological changes throughout the evolutionary history
144 of the major reptile lineages, the general morphologies of the skull roof and brain regions are
145 integrated across the entire clade. Second, as we wanted to test for a direct relationship between
146 frontal and forebrain and parietal and midbrain, we compared the anteroposterior positions of the
147 forebrain–midbrain boundary and the frontoparietal suture and demonstrated a significant correlation
148 between the two (P = 0.014), but with an unexpected pattern (Fig. 4, Table S2-S3). The best-fitting
149 linear regression model also included a categorical variable subdividing sampled taxa into two
150 groups ($P = 8.0^{-5}$). The first group includes non-archosaurian reptiles, stem reptiles, and non-
151 coelurosaurian archosaurs. In this sample, some of the taxa have a frontoparietal contact positioned
152 anterior to the forebrain–midbrain boundary. The second group consists of coelurosaurian dinosaurs,
153 including tyrannosaurs and crown birds. In these taxa, the forebrain–midbrain boundary and the
154 overlying suture are nearly aligned (Fig. S4). Conspicuously, alligators shift from a bird-like
155 configuration, with the brain and skull boundaries aligned, toward a non-coelurosaurian configuration,
156 with an offset between the two, during their ontogeny.
157 Thus, in coelurosaurs, compared with their successive sister taxa, the adult frontoparietal suture
158 shifts posteriorly relative to brain compartmental boundaries in a paedomorphic retention of the
159 original embryonic relationship (Fig. 1a, Fig. 2, Fig. 4, Fig. S4). We propose that the maintenance
160 of the posterior sutural position in adults is accompanied by the incorporation of additional and
161 more posteriorly located sources of skeletal precursor cells into the frontal, as suggested by cell-
162 lineage labeling experiments in chicken embryos[25]. The exact germ-layer origin of these cells is
163 unknown, but is most likely mesodermal, and may correspond to mesodermal precursors that
164 contribute to the parietal bone in non-avian reptiles. We note, however, that if this is the case,
165 there was no intrinsic morphological information contained in these precursors: the back of the
166 crown-avian frontal does *not* begin to look like the front of the ancestral dinosaurian parietal during
167 the evolutionary transition. Instead, despite altered proportions, it flares outward and has the same
168 proportional shape and articulations as other reptilian frontals (Fig. 1). The alternative explanation is
169 a novel contribution of more posteriorly located mesenchymal precursor cells, also resulting in a

largely mesodermal but potentially mixed composition of the "new" posterior part of the avian frontal. This configuration could explain the ongoing confusion and debate regarding the exact developmental origin of this structure. Some studies still suggest that the entire avian frontal is derived from neural crest cells, a migratory population of neuroectodermal derivation; other experiments suggest a mesodermal contribution[e.g. 17-18, 26]. Germ-layer origins have been used to argue that the avian frontal must be a fused frontoparietal because it contains both neural crest– and mesoderm-derived cells, and that the avian parietal, generally accepted as being mesodermally derived, is a postparietal. However, the central part of the interparietal of mammals, which is homologous to the ancestral amniote postparietal, has been described as being derived from neural crest[5]. This means that the avian frontoparietal hypothesis must invoke a shift in germ-layer origins, the avoidance of which was its core inspiration. Moreover, the germ-layer origins of cranial roof bones are more varied than previously reported. The parietal in mammals, for instance, is also reported to be of dual origin, with its central part derived from neural crest and its more lateral portions from mesoderm[3,6,27]. In amphibians, the parietal is reportedly either mesodermally derived (in the axolotl) or of mixed neural crest–mesodermal origin (in the fused frontoparietal element of *Xenopus* frogs)[17,26]. More notably still, the frontal of zebrafish, like that of chicken, is reported to be of composite neural crest and mesodermal origin[28]. This raises the possibility that a composite frontal is in fact the ancestral osteichthyan condition. Data from additional groups, especially from reptiles such as representatives of Crocodylia and Squamata, and from other non-tetrapod vertebrates, are needed to establish both the ancestral osteichthyan condition and the polarity of change.

The topology of all other structures in the avian head remains consistent with our conclusion that the entire enlarged avian frontal bone is homologous to the smaller frontal in more conservative groups, and that the constricted and rotated avian parietal is nonetheless homologous to the ancestral reptilian parietal. The positional relations of these two elements to other cranial structures, skeletal and non-skeletal, are conserved, both in adulthood and during ontogeny (Fig. 5). In particular, the parietal is always broadly flanked by the squamosals and contacts the supraoccipital posteriorly (Fig. 5). The eyes remain encircled by the frontals despite the greater size of eyes in crown birds, and

198 the pseudotemporalis or adductor internus group of the jaw muscles remains attached to the side of
199 the parietal, even as this bone becomes smaller and rotates to assume a more vertical orientation
200 (Fig. S5). The midbrain, including the optic lobes, remains subjacent to the parietal, though it is
201 shifted ventrally in crown birds. This conservation of topology stands in contrast to recent claims
202 that spatial relationships of the avian frontal and parietal are modified from the ancestral reptilian
203 condition[19,26]. Thus, in terms of adult anatomical homology, there is no evidence that the avian
204 frontal bone is a composite frontoparietal. Also, there is no evidence that the parietal is either a
205 "semiparietal" or a reacquired and radically transformed postparietal. A proposed novel contribution
206 to the posterior part of the avian frontal and a potential shift in germ-layer contribution appear to
207 have occurred without violating the structural homology of the bone.
208 The ontogenetic shift in developing alligator from close alignment of the forebrain–midbrain
209 boundary and frontoparietal suture to a displacement of those structures suggests that a decoupling
210 between the brain and skull roof occurs later during development, following what we hypothesized
211 to be an early close association of the initial ossifications of the skull roof with the divisions of
212 the brain. This bone-to-brain relationship had not previously been examined in embryos, so we used
213 contrast-stained CT scanning to simultaneously visualize the developing brain and skull roof in
214 *Alligator mississippiensis* and *Gallus gallus* (Fig. 6). We supplemented these data with a
215 developmental series of the lizard *Chalcides chalcides*. In all three taxa examined there is a direct,
216 one-to-one correspondence between the developing forebrain and the frontal bone primordium and
217 the developing midbrain and the parietal bone primordium. Moreover, this relationship can be seen
218 to exist in mouse and opossum, though it has attracted little comment[29]. Contrary to a recent
219 report based on 1937 data from de Beer[30], the initial parietal ossifications in chicken and mammals,
220 as well as in non-avian reptiles, appear in the same topological position relative to the brain, the
221 other bones of the skull (notably the squamosal), and the chondrocranium (Fig. 5). Our results
222 therefore support the notion that the brain plays an important role in patterning the skull roof.
223 **Conclusions**
224 We have shown that across the great change in brain size and shape in the evolution of birds from
225 the reptile ancestor, the skull roof tracks the brain early in ontogeny and then becomes decoupled,

with a truncation of this decoupling occurring in Coelurosauria. The skull roof is remarkably conservative across reptiles, and we found no evidence that the avian parietal is anything other than a structure homologous to the ancestral reptilian parietal. The novel and dramatic posterior expansion of the avian frontal may be stimulated by the contribution of additional skeletal progenitor cells, most likely of mesodermal origin. Overall evidence indicates that this expansion of the frontal is not a product of fusion with the parietal. Finally, we have shown for the first time a one-to-one correspondence in embryos between major parts of the brain and the early ossifications of the skull-roof elements, a condition likely ancestral to all amniotes and possibly to all osteichthyans. This relationship, however, is dynamic during ontogeny, and the nature of the relation in adults shifts during the evolution of the avian lineage. This result serves as an example of character non-independence: the enlargement of the brain had widespread consequences on surrounding cranial elements, affecting the entire architecture of the skull. It also highlights the fact that developmental data by themselves are not sufficient to determine homology and must be interpreted within a phylogenetic framework provided by the fossil record and comparative morphology. Finally, it raises the question of whether the intimate association of the frontal and parietal with the brain, which is known to act as a major signaling center at least in terms of facial development, is the reason for their universal conservation in bony vertebrates; and whether the repeated losses of posterior cranial elements such as the postparietal, tabulars, and supratemporals have to do with their more peripheral positions with respect to an influential source of molecular developmental patterning information.

Acknowledgments: We are grateful to Emily J. Rayfield, Andrew R. Cuff, Yoshitsugu Kobayashi, Sankar Chatterjee, Alan Turner, and Larry Witmer for providing CT data and to Greg Watkins-Colwell for assisting with cleared and stained squamate embryo specimens, as well as Daniel Smith for their imaging. Farish A. Jenkins, Jr., Jacques A. Gauthier, Günter Wagner and Guillermo Navalon provided useful discussion. Elizabeth M. Sefton, Hillary Maddin, and James Hanken commented on the early stages of the work as it was underway. All Yale authors are supported by funds from Yale University. D.J.F. is supported in part by NSF DDIG DEB 1500798 to B.-A.S.B

and D.J.F. A.P. is supported by an NSF Postdoctoral Research Fellowship in Biology. J.C. was partially funded by an NSF Graduate Research Fellowship and by NSF DDIG DEB 1501690. A.A. was supported by NSF grant 1257122, the Templeton Foundation grant RFP-12-0 and by funds from Imperial College London. G.S.B, A.M.B., and M.A.N are supported in part by NSF DEB 1457181.

Contributions: B-A.S.B. and A.A. conceived and planned the research. M.F., A.C.P., M.H., E.H., G.S.B., A.M.B., J.C., Z.M., D.J.F. and B.-A.S.B. scanned specimens and performed segmentation. M.F., N.M.K., A.C.P., M.H., and B.-A.S.B. placed landmarks and performed morphometric analyses. M.F. and N.M.K. performed correlation tests. M.F., N.M.K., A.C.P., M.H., E.H., G.S.B., T.B.R., A.A., and B.-A.S.B., wrote the paper. M.A.N. and R.M.S. provided CT data and assisted in anatomical interpretation.

Materials and Methods

Original CT scan data of the taxa included in this analysis were acquired at the University of Texas High-Resolution X-Ray Scanning Facility (UTCT), at the University of the Witwatersrand Bernard Price Institute for Palaeontological Research (BPI), and at the Harvard Center for Nanoscale Systems (CNS). Endocasts of the brain and the skull elements were segmented using the software VGStudio. The taxa stem-ward of *Proterosuchus* do not ossify the anteroventral portion of their braincases, such that endocasts were necessarily less complete. However, we only analyzed those parts of the endocasts that were directly in contact with the skull roof (Fig. S1). The braincases of the coelurosaur *Garudimimus* and of the stem archosaur *Euparkeria* were partially disarticulated and required digital re-articulation. The restoration was performed in VGStudio. Normal developmental series for *Gallus gallus* (four stages, including E12, E15, E17 and E19), *Alligator mississippiensis* (four stages, including E32, E40, E46 and hatchling) and *Chalcides chalcides* (YPM R 15063) were included in the analyses for investigating the pattern of skull ossification and to test the one-to-one correlation between frontal and forebrain on the one hand and parietal and midbrain on the other. Embryos were stained in a 5% (by mass) phosphomolybdic acid, before CT scanning them.

The 3D configurations of landmarks were digitized with VGStudio on the CT scan data for all the taxa included in this study. Only one side of the braincase was landmarked. The right or left side of the braincase was chosen on the base of the presence or absence of deformation, quality of preservation and completeness of the specimen. In the case of *Garudimimus*, we placed the landmarks on the right side of the braincase, because it was less deformed as suggested by the more rounded morphology of the orbit[31].

Generalized Procrustes analysis (GPA)[32] was applied in order to remove information relating to the location, size and orientation of the landmark configurations. The three-dimensional coordinates of landmarks were subjected to a full GPA, given the reduced sensitivity to outliers of this approach[33]. Analysis were performed using MorphoJ v. 1.03b[34], which automatically reflects specimens that were digitized on alternative sides. Major patterns of morphological variability were then extracted using Principal component analysis (PCA) on the Procrustes-aligned coordinates.

Delineation of clusters (that is, groups of organisms with similar morphology) was done using *k*-means clustering[35]. The method aims at partitioning all observations into *k* groups such that the sum of squares from all observations to their assigned cluster centers is minimized. Given the heuristic nature of the method, results shown derive from initiating the process from 1000 different randomly located cluster centers. Number of clusters in each case was determined using R package *NbClust*[36] that provides 30 metrics to evaluate the optimal number of clusters in a dataset. In all cases (Fig. 3, Fig. S2), clustering was performed using all principal components that explained a variance > 1%, and the number of clusters chosen was that supported by the majority of metrics.

We used the R package *geomorph*[37-38] to test the hypothesis of modularity between skull roof and brain. The Covariance Ratio (CR) was chosen as a measure to characterize the degree of covariance between these two *a priori* defined modules[39]. CR was preferred over the widely used RV coefficient[40], because it is not influenced by attributes of the data such as the sample size and the number of variables[39]. Briefly, this metric represents the overall covariation between defined modules relative to the overall covariation found within them. For random sets of variables, the CR coefficient has an expected value of one; significant departures towards lower values are indicative of modularity. Significance was tested using a permutation test which randomly reassigns landmarks

into groups of equal size as the original partitions, and calculates the CR value for the generated subdivisions of landmarks. The degree of modularity between the skull roof and the brain was tested using: A) the full set of digitized landmark configurations (n = 21), and B) only those corresponding to adult specimens (n = 17). The sampling employed in the first set leads to difficulties interpreting the results, since they are determined by a mix of ontogenetic and evolutionary signals of integration across structures[41]. Therefore, results in the main text correspond to those of set B, which only assesses the degree of evolutionary integration. In both cases, we performed 10^4 permutations, and *P* values were empirically calculated as the fraction of permutations with CR values lower than the original. The analysis of set A (i.e., including the landmark configurations of the chicken and crocodile embryos), results in a significant degree of modularity between skull roof and brain (CR = 0.967, $P = 0.031$). This might provide further evidence for the morphological decoupling between the two structures during ontogeny, as discussed in the main text, but once again caution should be taken when interpreting this result.

In order to further explore the morphological covariance between skull roof elements and brain regions, we measured the relative positions of the fronto-parietal and forebrain-midbrain sutures. Sagittal sections of the braincase and brain of all adults were extracted from the CT scans using VGStudio. Images were then imported into tpsDIG2 v. 2.22[42], where the distance between the anterior tip of the olfactory bulbs and the foramen magnum was measured as the curved line joining those points along the internal side of the skull. This measure was used as a proxy for the overall skull roof length. The relative positions of both fronto-parietal and fore-mid brain sutures along the same line was quantified as their distance to the tip of the olfactory bulbs divided by the overall length, thus eliminating differences due to specimen size.

A relationship between the positions of the fronto-parietal suture and forebrain-midbrain suture was explored using a combination of ordinary and phylogenetic linear models. For the latter, a phylogenetic supertree was created in the software Mesquite v 3.04[43]. The topology of the tree was based on Pinheiro et al.[44] for early diapsids and Archosauromorpha, Gauthier et al.[45] for Squamata, Nesbitt[46] for Archosauriformes and Archosauria, Carrano et al.[47] for Tetanurae, Brusatte et al.[48] for Coelurosauria and Prum et al.[49] for Aves. A time-scaled version of the phylogenetic tree was built

using the calibration method described in Brusatte[50]. First and last appearances of all fossil taxa were recorded from the primary literature (See Table S2 for ages of the taxa and corresponding citations) and used to estimate the time of divergence of the clades represented in the analysis. This was done using the timePaleoPhy function in the R package *paleotree*[51]. Molecular estimates for the divergence of crown clades were drawn from Shedlock & Edwards[52] and Prum *et al.*[49], and used to constrain minimum ages for the respective nodes. To account for uncertainty in both branch length estimates and phylogenetic relationships among paravian lineages, 100 different trees were generated by assigning an age for each taxon through random sampling between its first and last appearance in the fossil record, as well as randomly resolving the polytomy at the base of Paraves. The resulting 100 trees were subsequently used in all following analysis.

We considered three increasingly complex least-squares regression models: a model of simple allometry, a model incorporating different intercepts for coelurosaur and non-coelurosaur diapsids but with same slope, and a model with both different intercepts and slopes (shown in Table S3 as models A, B and C, respectively). Division of the included taxa into a coelurosaur and a non-coelurosaur group was applied on the base of the shift in the organization of braincase-brain found through the analyses performed in this study. As already stated, ordinary least squares (OLS) and phylogenetic generalized least squares (PGLS) approaches of these three models were performed (for the later, we used the R package *caper*.[53]). A dummy variable representing clade membership was coded and included as categorical factor[as in.54-55]. Given the sensitivity of methods to deviations from a strict Brownian motion model[56], branch length modifying parameters (λ, δ and κ[57-58]) were simultaneously estimated along the regression parameters, following the recommendations of Revell[59]. For each of the three models, the fit of the OLS and 8 different PGLS (resulting from all combinations including the estimation of branch length modifying parameters, see Table S3) were compared using AIC weights, given that different scenarios are not nested within each other. On the other hand, the fit of progressively more complex models (i.e. simple allometry, allometry with clade-specific intercepts and allometry with clade-specific intercepts and slopes) was analyzed using log-likelihood ratio tests (LRT). The model with the best fit was considered to be the one with the lowest AIC value overall.

Several lines of evidence favored the OLS model including different intercepts but equal slopes for the two clades as the preferred one, the results of which are shown in Fig. 4 of the main text**.** This model had the overall smallest AIC value, and represented a significant improvement with respect to the OLS simple allometry (P = 0.000); while the addition of different slopes for each clade was not considered to further improve the model (P = 0.394). This was also confirmed through the use of a partial F-test (F = 0.57, P = 0.464). In fact, the regression residuals were found to lack phylogenetic signal, with a value of K = 0.20[60] and λ = 0.73 (P = 0.64 and 0.37, respectively, using 100 simulations with function phylosig of R package *phytools*[61]). Under such situation, OLS approaches have an estimation accuracy substantially higher than PGLS[59]. Allowing for the simultaneous estimation of branch length modifying parameters also confirmed this result. The second best model including a clade effect with equal slopes is a PGLS approach that includes a parameter λ = 0 and δ = 0.019, transforming the tree into a star phylogeny and (almost completely) homogenizing terminal branch lengths. This transformation effectively eliminates residual correlation due to shared evolutionary history from the variance-covariance matrix of the linear model (analogous to the $PGLS_{\lambda}$ approach discussed by Revell[59], with the addition of a parameter $\delta \approx 0$ to eliminate differences in terminal branch lengths), resulting in an approach equivalent to an OLS.

Data availability. CT data are in part publicly available in www.digimorph.org. The remnant CT data are available through the corresponding author, upon reasonable request. Landmarks are available as supplementary files in www.nature.com.

References cited

1. Richtsmeier, J. T. & K. Flaherty. Hand in glove: brain and skull development and dysmorphogenesis. *Acta Neuropathologica*, **125**, 469-489 (2013).
2. Richtsmeier, J. T., et al. Phenotypic integration of neurocranium and brain. *Journal of Exper. Zool.* **306**, 360-378 (2006).

3. Koyabu, D. *et al.* Mammalian skull heterochrony reveals modular evolution and a link between cranial development and brain size. *Nature comms*, **5** (2014).
4. Rowe, T. Evolution of nervous systems in *The emergence of mammals* Kaas 2e. vol. 2, pp. 1-52. Oxford: Elsevier (2017).
5. Jiang, X., S. Iseki, R. E. Maxon, H. M. Sucov, & G. M. Morriss-Kay. Tissue origins and interactions in the mammalian skull vault. *Develop. Biology*, **241**, 106-116 (2002).
6. Morriss□Kay, G. M. Derivation of the mammalian skull vault. *Journal of anatomy*, **199**, 143-151 (2001).
7. Noden, D. M. Interactions and fates of avian craniofacial mesenchyme. *Development*, **103**, 121-140 (1988).
8. Marcucio, R. S., Young, N. M., Hu, D., & Hallgrimsson, B. Mechanisms that underlie co□ variation of the brain and face. *Genesis*, **49**, 177-189 (2011).
9. Marcucio, R. S., Cordero, D. R., Hu, D., & Helms, J. A. Molecular interactions coordinating the development of the forebrain and face. *Develop. biology*, **284**, 48-61 (2005).
10. Hu, D., & Marcucio, R. S. A SHH-responsive signaling center in the forebrain regulates craniofacial morphogenesis via the facial ectoderm. *Development*, **136**, 107-116 (2009).
11. Bhullar, B. A. S. *et al.* A molecular mechanism for the origin of a key evolutionary innovation, the bird beak and palate, revealed by an integrative approach to major transitions in vertebrate history. *Evolution*, **69**, 1665-1677 (2015).
12. Abzhanov, A., Protas, M., Grant, B. R., Grant, P. R., & Tabin, C. J. Bmp4 and morphological variation of beaks in Darwin's finches. *Science*, **305**, 1462-1465 (2004)
13. Balanoff, A. M., Bever, G. S., Rowe, T. B., & Norell, M. A. Evolutionary origins of the avian brain. *Nature*, **501**, 93-96 (2013).
14. Hopson, J. A. Relative brain size and behavior in archosaurian reptiles. *Ann. Rev. Ec. System.*, **8**, 429-448 (1977).
15. Marugán□Lobón, J., Watanabe, A., & Kawabe, S. Studying avian encephalization with geometric morphometrics. *Journal anat.*, **229**, 191-203 (2016).

16. Couly, G. F., P. M. Coltey, & N. M. Le Douarin. The triple origin of skull in higher vertebrates: a study in the quail-chick chimeras. *Development*, **117**, 409-429 (1993).
17. Maddin, H. C., Piekarski, N., Sefton, E. M., & Hanken, J. Homology of the cranial vault in birds: new insights based on embryonic fate-mapping and character analysis. *Roy. Soc. Open Science*, **3**, 160356 (2016).
18. Noden, D. M., & Trainor, P. A. Relations and interactions between cranial mesoderm and neural crest populations. *Jour.l of anat.*, **207**, 575-601 (2005).
19. Pinna, M. C. Concepts and tests of homology in the cladistic paradigm. *Cladistics*, **7**, 367-394 (1991)
20. Bhullar, B. A. S. *et al.* How to make a bird skull: Major transitions in the evolution of the avian cranium, paedomorphosis, and the beak as a surrogate hand. *Integ. Comp. Biology*, icw069 (2016).
21. Bhullar, B. A. S. *et al.* Birds have paedomorphic dinosaur skulls. *Nature*, **487**, 223-226 (2012).
22. Gauthier, J., Estes, R. & de Queiroz, K. in *Phylogenetic Relationships of the Lizard Families: Essays Commemorating Charles L. Camp* (eds. Estes, R. & Pregill, G.) 15–98 (Stanford University Press, 1988).
23. Nesbitt, S. J. The early evolution of archosaurs: Relationships and the origin of major clades. *Bull. Am. Museum Nat. Hist.* **352,** 1–292 (2011)
24. Butler, R., Sullivan, C. & Ezcurra, M. New clade of enigmatic early archosaurs yields insights into early pseudosuchian phylogeny and the biogeography of the archosaur radiation. *BMC* **14**, 128 (2014)
25. Abzhanov, A., Rodda, S. J., McMahon, A. P. & Tabin, C. J. Regulation of skeletogenic differentiation in cranial dermal bone. *Development* **134,** 3133–3144 (2007)
26. Gross, J. B. & Hanken, J. Review of fate-mapping studies of osteogenic cranial neural crest in vertebrates. *Dev. Biol.* **317,** 389–400 (2008)
27. Chai, Y., Jiang, X., Ito, Y., Bringas, P. & Han, J. Fate of the mammalian cranial neural crest during tooth and mandibular morphogenesis. *Development* **127**, 1671–1679 (2000)

448 28. Kague, E. *et al.* Skeletogenic fate of zebrafish cranial and trunk neural crest. *PLoS One*, **7**,
449 e47394 (2012).
450 29. Clark, C. & Smith, K. Cranial osteogenesis in Monodelphis domestica (Didelphidae) and
451 Macropus eugenii (Macropodidae). *J. Morphol.* **215**, 119-149 (1993)
452 30. de Beer, G. R. *The Development of the Vertebrate Skull*. (Clarendon Press, 1937)
453 31. Cuff, A. R., & Rayfield, E. J. Retrodeformation and muscular reconstruction of
454 ornithomimosaurian dinosaur crania. *PeerJ*, **3**, e1093 (2015).
455 32. Dryden IL, Mardia KV. Statistical shape analysis. London: Wiley (1998).
456 33. Rohlf FJ. Shape statistics: Procrustes superimpositions and tangent spaces. J Classification **16**,
457 197–223 (1999).
458 34. Klinberger CP MorphoJ: an integrated software package for geometric morphometrics. Mol Ecol
459 Resour **11**, 353–357 (2011)
460 35. Hartigan, J. A., & Wong, M. A. Algorithm AS 136: A k-means clustering algorithm. *Journal of*
461 *the Royal Statistical Society. Series C (Applied Statistics)*, **28**, 100-108 (1979).
462 36. Charrad, M., Ghazzali, N., Boiteau, V., Niknafs, A., & Charrad, M. M. Package 'NbClust'. *J.*
463 *Stat. Soft*, **61**, 1-36 (2014).
464 37. Adams, D. C., & Otárola□Castillo, E. geomorph: an R package for the collection and analysis of
465 geometric morphometric shape data. *Methods in Ecology and Evolution*, **4**, 393-399 (2013).
466 38. Adams, D. C., & Collyer, M. L. Permutation tests for phylogenetic comparative analyses of
467 high□dimensional shape data: What you shuffle matters. *Evolution*, **69**, 823-829 (2015).
468 39. Adams, D. C. Evaluating modularity in morphometric data: challenges with the RV coefficient
469 and a new test measure. *Methods in Ecology and Evolution* **7**, 565–572 (2016).
470 40. Klingenberg, C. P. Morphometric integration and modularity in configurations of landmarks:
471 tools for evaluating a priori hypotheses. *Evolution & development*, **11**, 405-421 (2009).
472 41. Klingenberg, C. P. Morphological integration and developmental modularity. *Annual review of*
473 *ecology, evolution, and systematics*, **39**, 115-132 (2008).
474 42. Rohlf, F. J. The tps series of software. *Hystrix, the Italian Journal of Mammalogy*, **26**, 9-12
475 (2015).

476 43. Maddison, W. P., & Maddison, D. R. Mesquite: a modular system for evolutionary analysis.
477 Version 3.04, http://mesquiteproject. Org (2015).
478 44. Pinheiro, F. L., França, M. A., Lacerda, M. B., Butler, R. J., & Schultz, C. L. An exceptional
479 fossil skull from South America and the origins of the archosauriform radiation. *Scientific*
480 *reports*, **6** (2016).
481 45. Gauthier, J. A., Kearney, M., Maisano, J. A., Rieppel, O., & Behlke, A. D. Assembling the
482 squamate tree of life: perspectives from the phenotype and the fossil record. *Bulletin of the*
483 *Peabody Museum of Natural History*, **53**, 3-308 (2012).
484 46. Nesbitt, S. J. The early evolution of archosaurs: relationships and the origin of major clades ***Bull.***
485 ***Am. Museum Nat. Hist.*** **352,** 1–292 (2011).
486 47. Carrano, M. T., Benson, R. B., & Sampson, S. D. The phylogeny of Tetanurae (Dinosauria:
487 Theropoda). *Journal of Systematic Palaeontology*, **10**, 211-300 (2012).
488 48. Brusatte, S. L., Lloyd, G. T., Wang, S. C., & Norell, M. A. Gradual assembly of avian body plan
489 culminated in rapid rates of evolution across the dinosaur-bird transition. *Current Biology*, **24**,
490 2386-2392 (2014).
491 49. Prum, R. O., ***et al.*** comprehensive phylogeny of birds (Aves) using targeted next-generation
492 DNA sequencing. *Nature*, **526**, 569-573 (2015).
493 50. Brusatte, S. L. Calculating the tempo of morphological evolution: rates of discrete character
494 change in a phylogenetic context. In *Computational paleontology* (pp. 53-74) (2011).
495 51. Bapst, D. W. paleotree: an R package for paleontological and phylogenetic analyses of
496 evolution. *Methods in Ecology and Evolution*, **3**, 803-807 (2012).
497 52. Shedlock, A. M., & Edwards, S. V. Amniotes (amniota). *The time tree of life*, 375-379 (2009).
498 53. Orme, D. ***et al.*** The caper package: comparative analysis of phylogenetics and evolution in R v.
499 0.5. *Availabe online at: http://cran. r-project. org/web/packages/caper/index. Html* (2013).
500 54. Lavin, S. R., Karasov, W. H., Ives, A. R., Middleton, K. M., & Garland Jr, T. Morphometrics of
501 the avian small intestine compared with that of nonflying mammals: a phylogenetic
502 approach. *Physiological and biochemical zoology*, **81**, 526-550 (2008).

55. Gartner, G. E., *et al.* Phylogeny, ecology, and heart position in snakes. *Physiological and Biochemical Zoology*, **83**, 43-54 (2009).
56. Diaz-Uriarte, R., & Garland, T. Testing hypotheses of correlated evolution using phylogenetically independent contrasts: sensitivity to deviations from Brownian motion. *Systematic Biology*, **45**, 27-47 (1996).
57. Pagel, M. Inferring evolutionary processes from phylogenies. *Zoologica Scripta*, **26**, 331-348 (1997).
58. Pagel, M. Inferring the historical patterns of biological evolution. *Nature*, **401**, 877-884 (1999).
59. Revell, L. J. Phylogenetic signal and linear regression on species data. *Methods in Ecology and Evolution*, **1**, 319-329 (2010).
60. Blomberg, S. P., Garland Jr, T., & Ives, A. R. Testing for phylogenetic signal in comparative data: behavioral traits are more labile. *Evolution*, **57**, 717-745 (2003).
61. Revell, L. J. phytools: an R package for phylogenetic comparative biology (and other things). *Methods in Ecology and Evolution*, **3**, 217-223 (2012).

Figure 1. Summary of skull roof evolution and relationship to soft tissue structures in Reptilia. a, To the left, phylogenetic tree showing presence (orange) or absence (green) of separate postparietal. The postparietal is ancestral for Reptilia and was lost several times within it, notably at the base of crown Archosauria with one reversal in *Gracilisuchus*. To the right, dorsal views of the segmented skull roof and brain endocast of selected taxa, anterior to the left, demonstrating the uniformly small size of the postparietal and the gradual transformation of the skull roof toward the avian lineage. b, Sagittal cutaway through the skull of the stem crocodylian *Gracilisuchus stipanicorum* including brain endocast, showing the relationship of the skull roof bones to the endocranium and the separation of the postparietal from the brain by the skull roof, braincase, and nuchal musculature. Anterior to the left. c, Sagittal cutaway as in b, but of near-hatching (E46) *Alligator*

mississippiensis, showing relation of contrast-stained brain and nuchal musculature to skull roof and braincase. d, Sagittal cutaway of contrast-stained chicken, *Gallus gallus*, showing relation of contrast-stained brain and nuchal musculature to skull roof and braincase. Frontal in fuchsia; parietal in green; postparietal in orange; brain endocast in blue.

Figure 2. Oblique dorsolateral views of skull roofs, braincases, and brain endocasts of selected newly sampled fossil taxa, anterior to the lower left. Skull elements are cut along the sagittal plane leaving only the right sides, but endocasts are entire. These are the first reported endocasts of the early stem reptile *Youngina*, the stem archosaur *Proterosuchus*, the near-crown stem archosaur *Euparkeria*, the stem crocodylian *Gracilisuchus*, and the early-diverging dinosaur *Herrerasaurus*. The postparietal, where present, is uniformly small and restricted to a superficial, posterior position on the skull. The skull roof in *Zanabazar* is characteristic of coelurosaurs in that the frontoparietal suture is shifted backward, closer to the forebrain–midbrain boundary.

549 **Figure 3.** 3D geometric morphometric principal component analyses (PCAs) of brains and skull
550 roofs in reptiles. a, Phylogenetic tree showing included taxa and indicating color coding in plots. b,
551 PCA plot including brain and skull roof landmarks. c, PCA plot including only skull roof
552 landmarks. d, PCA plot including only brain landmarks. Taxa are grouped following k-means
553 clustering with automatic selection of the appropriate number of clusters. A cluster of all avialan
554 specimens is always found, sometimes also including alligator embryos. The remaining non-avialan
555 reptiles are recovered as one cluster when analyzing brain morphology, or two clusters when
556 including skull roof morphology, with allosauroids exhibiting a divergent morphology. Gray cluster is
557 adult non-dinosaurian reptiles and non-avialan reptiles. Red cluster is Avialae. Blue arrows indicate
558 alligator ontogeny. Red arrows indicate chicken ontogeny. See Supplementary Information for silhouette
559 sources. Silhouettes from http://phylopic.org.
560
561
562

Figure 4. Relationship between the position of frontoparietal suture and position of forebrain–midbrain boundary. Results derive from a linear model including clade as a categorical dummy variable and equal slopes (P=3.0^{-4}, R^2=0.69). Upper black line is regression for non-coelurosaurian reptiles, lower line is the regression for coelurosaurs. Diameters of the dots represent relative distance between the two sutures. For a comparison with phylogenetic generalized-least squares approaches, as well as method justification, refer to the Materials and Methods session. Embryos are plotted, although only adults were used in the analysis. Blue indicates all non-coelurosaur taxa. Red indicates the coelurosaur clade. Gray indicates alligator and chicken embryos and their ontogenetic trajectories. Silhouettes from http://phylopic.org.

Figure 5. Ossification of cranial elements in (a), (b) embryonic alligator (sample size=10) and (c), (d) embryonic chicken (sample size=10). Frontals are fuchsia, parietals green, and in the rightmost column, squamosals are turquoise, supraoccipitals yellow, and exoccipitals red. Note that the parietal primordia in E32 alligators and E15 chickens are similar in form and relative location, taking into account the compressed and rotated temporal region of the cranium in birds. Note also the homologous topological position of the parietals in both taxa with respect to the squamosals, flanking them and the supraoccipitals and exoccipitals behind.

Figure 6. Above: Ossification of the frontal (pink) and parietal (green) over the brain (blue) in embryonic alligator (sample size=6) and chicken (sample size=6), with the eyes (white) and nuchal musculature (orange) shown in place. Below: Ossification of the frontal and parietal in an embryonic *Chalcides* lizard (Squamata) (sample size=2). In all of these taxa, bracketing Reptilia, the frontal first forms over the forebrain (fb) and the parietal first over the midbrain (mb).

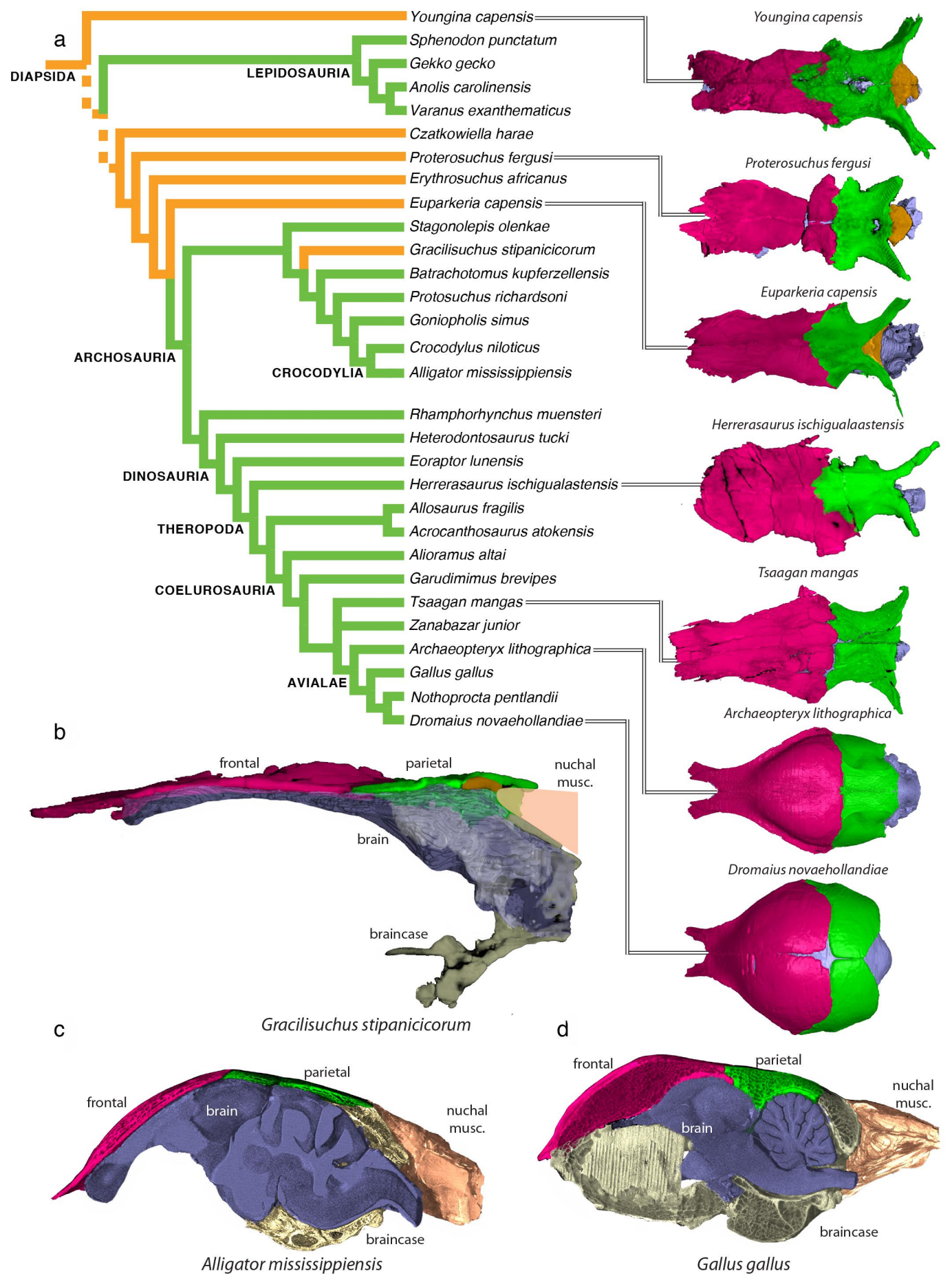
a
DIAPSIDA
LEPIDOSAURIA
ARCHOSAURIA
CROCODYLIA
DINOSAURIA
THEROPODA
COELUROSAURIA
AVIALAE
Youngina capensis
Sphenodon punctatum
Gekko gecko
Anolis carolinensis
Varanus exanthematicus
Czatkowiella harae
Proterosuchus fergusi
Erythrosuchus africanus
Euparkeria capensis
Stagonolepis olenkae
Gracilisuchus stipanicicorum
Batrachotomus kupferzellensis
Protosuchus richardsoni
Goniopholis simus
Crocodylus niloticus
Alligator mississippiensis
Rhamphorhynchus muensteri
Heterodontosaurus tucki
Eoraptor lunensis
Herrerasaurus ischigualastensis
Allosaurus fragilis
Acrocanthosaurus atokensis
Alioramus altai
Garudimimus brevipes
Tsaagan mangas
Zanabazar junior
Archaeopteryx lithographica
Gallus gallus
Nothoprocta pentlandii
Dromaius novaehollandiae
Youngina capensis
Proterosuchus fergusi
Euparkeria capensis
Herrerasaurus ischigualaastensis
Tsaagan mangas
Archaeopteryx lithographica
Dromaius novaehollandiae
b
frontal
parietal
nuchal musc.
brain
braincase
Gracilisuchus stipanicicorum
c
frontal
parietal
brain
nuchal musc.
braincase
Alligator mississippiensis
d
frontal
parietal
nuchal musc.
brain
braincase
Gallus gallus

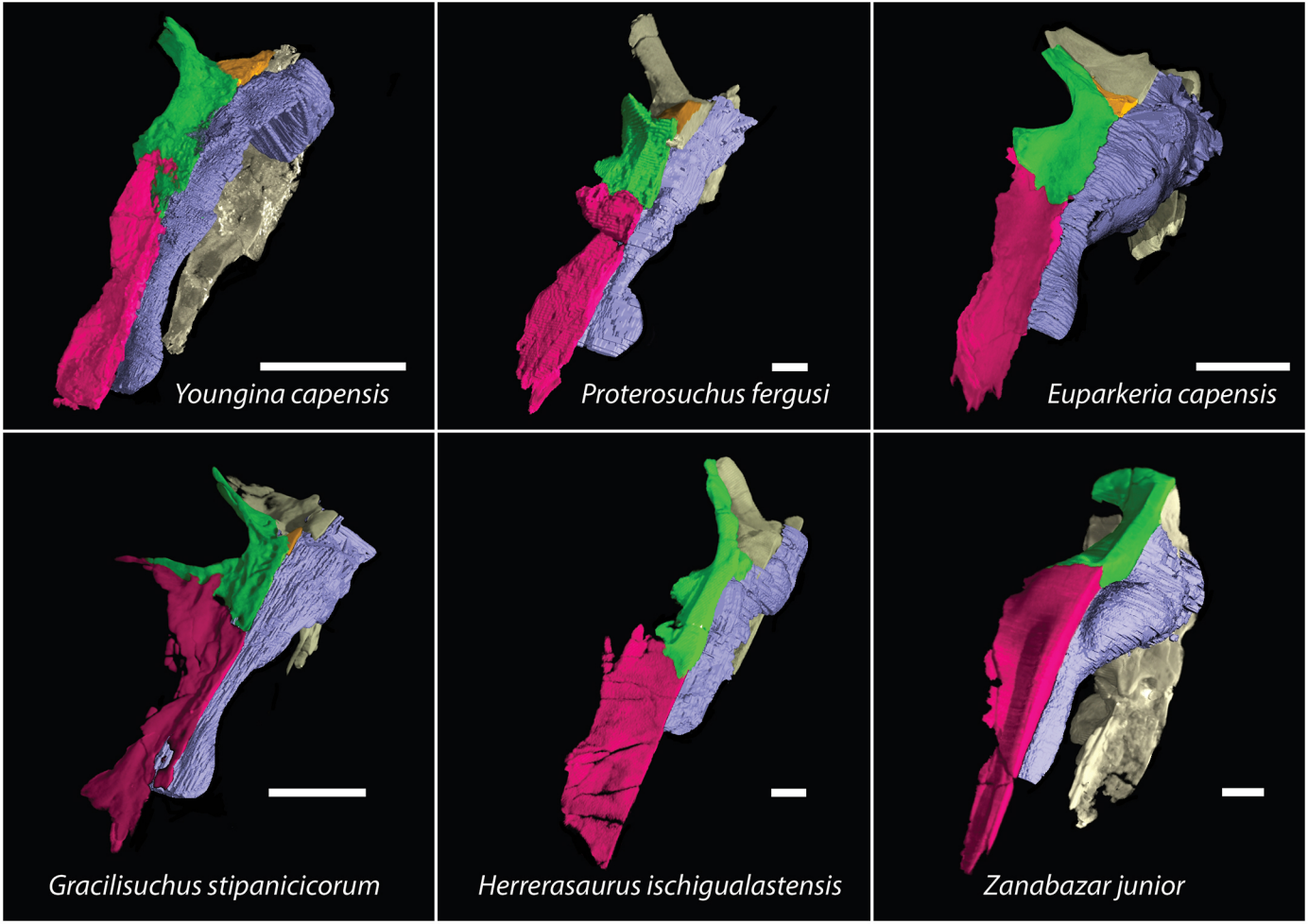
Youngina capensis
Proterosuchus fergusi
Euparkeria capensis
Gracilisuchus stipanicicorum
Herrerasaurus ischigualastensis
Zanabazar junior

a

Youngina
Anolis
Proterosuchus
Euparkeria
Gracilisuchus
Alligator
Herrerasaurus
Allosaurus
Acrocanthosaurus
Alioramus
Garudimimus
Tsaagan
Zanabazar
Archaeopteryx
Gallus
Dromaius
Nothoprocta

b

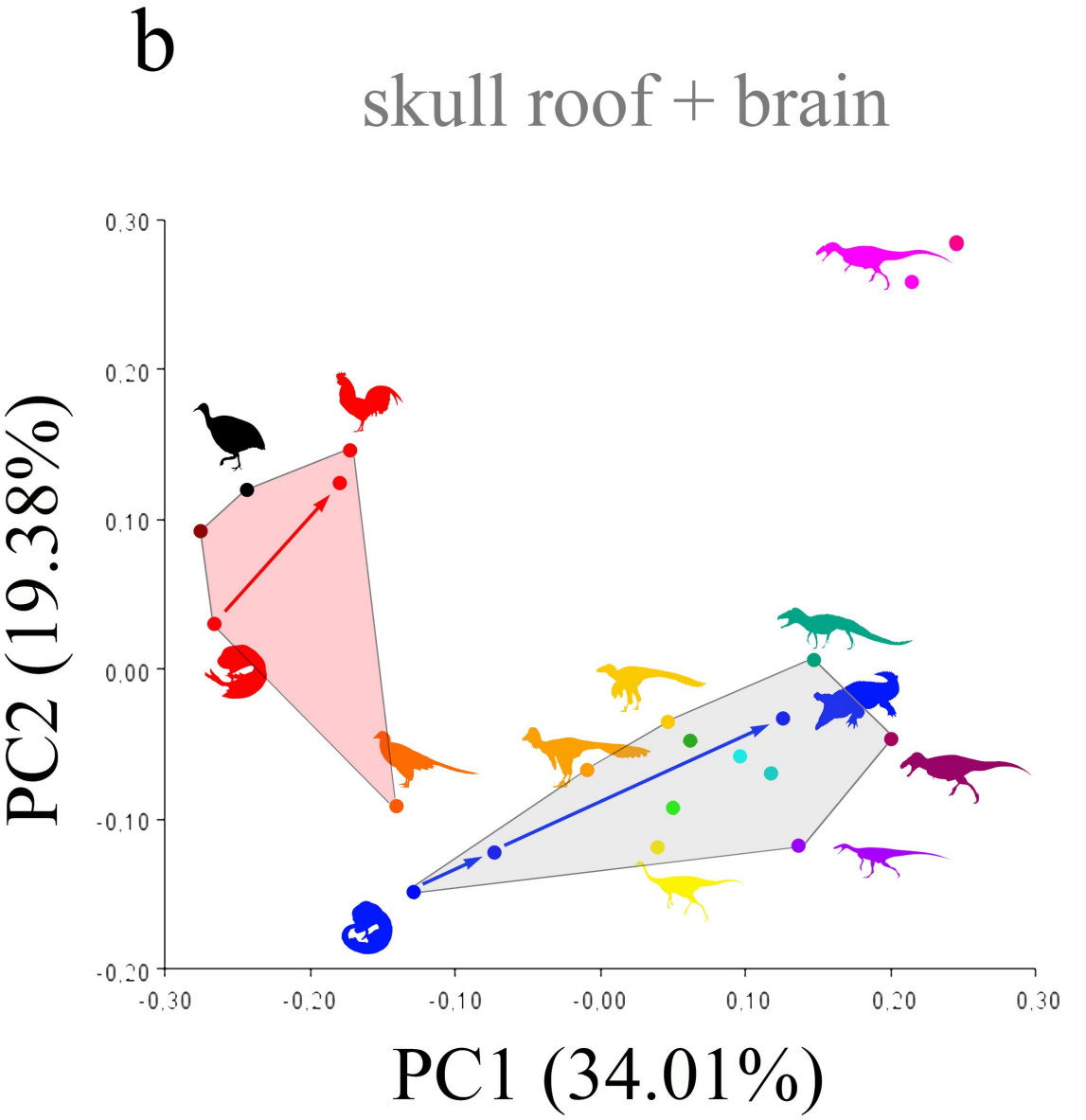

c

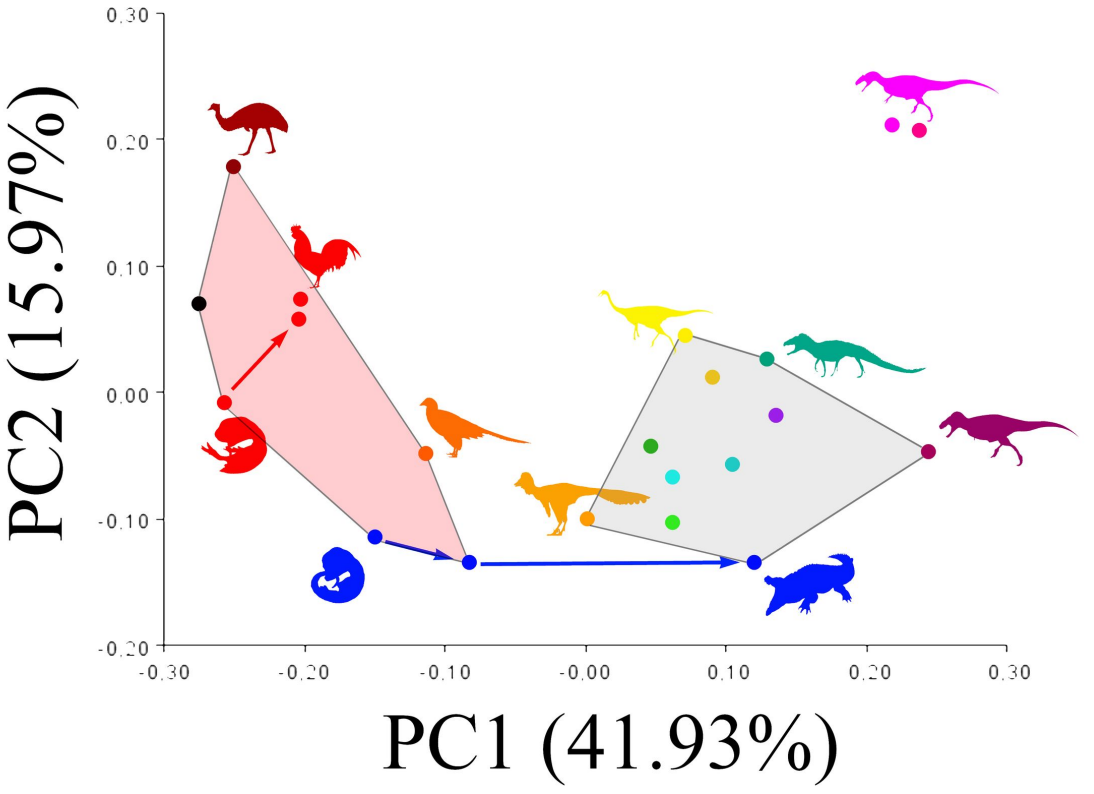

d

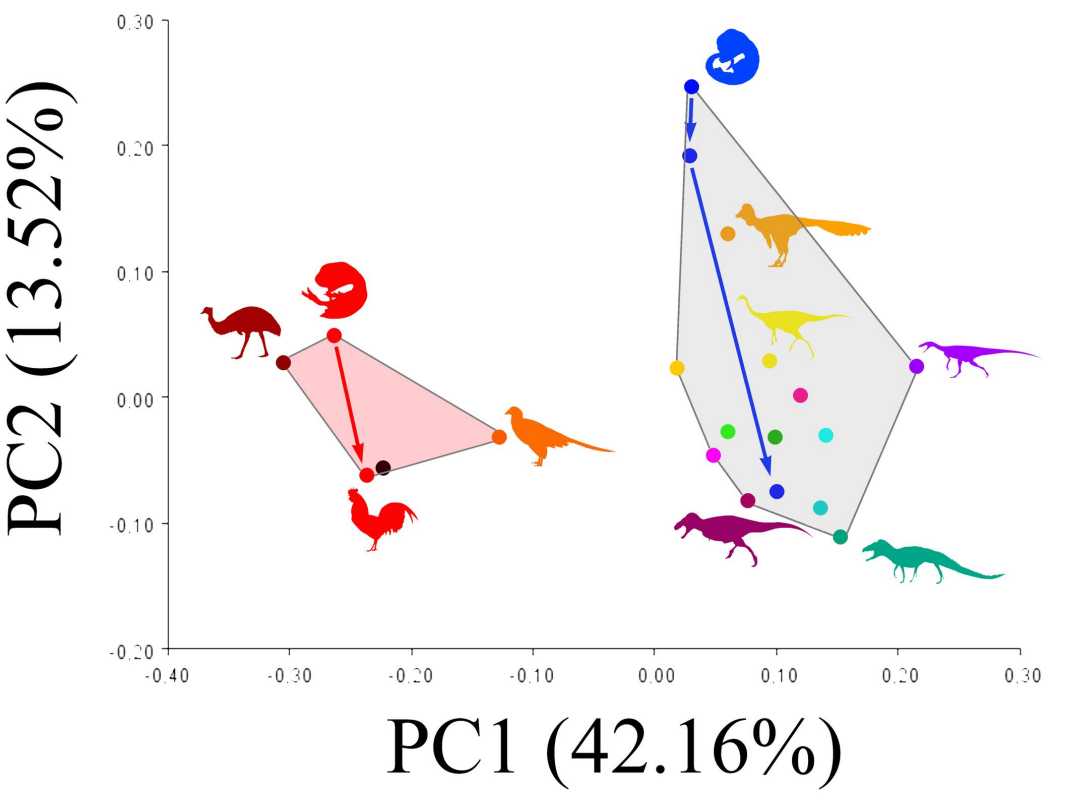

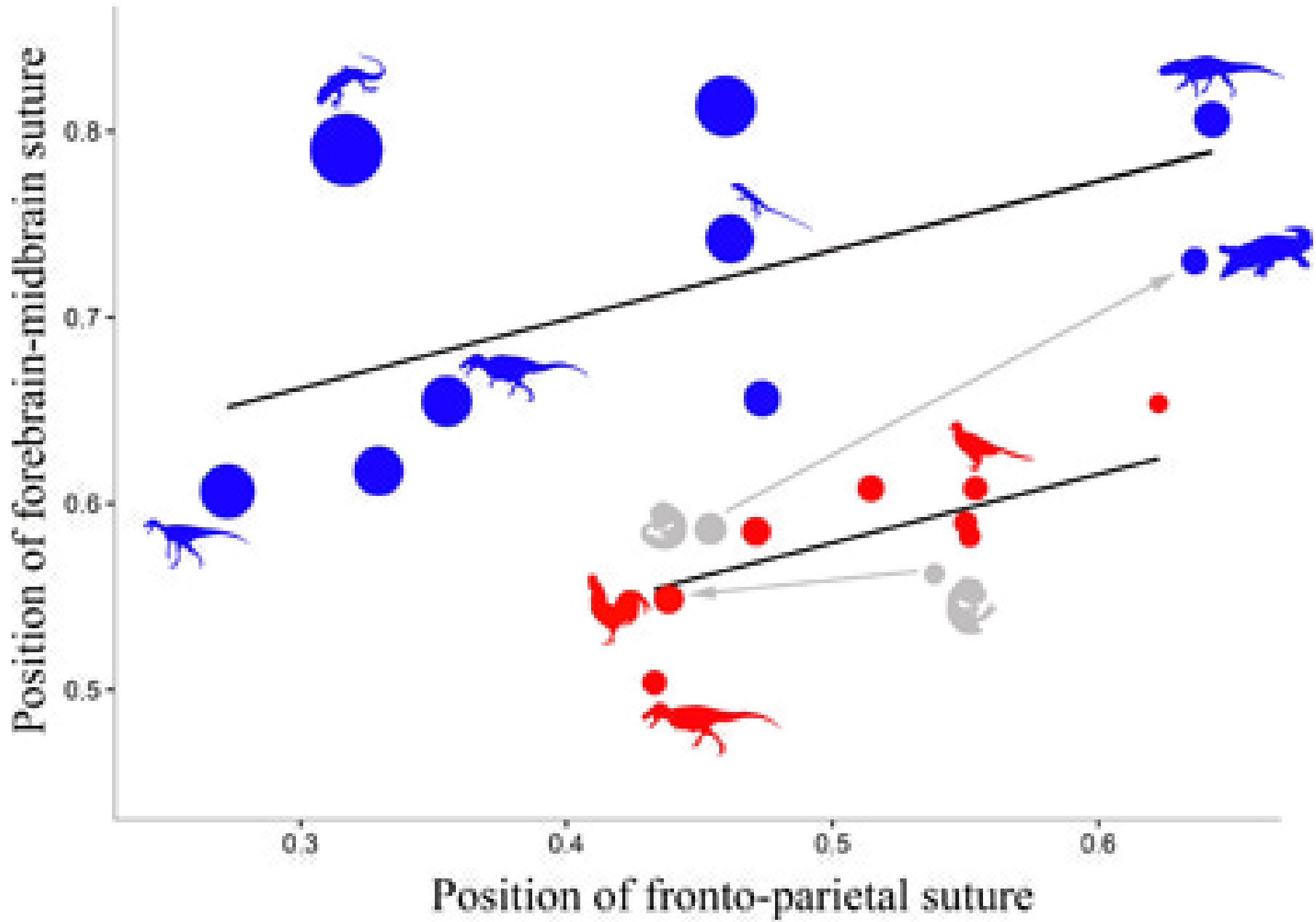
Position of forebrain-midbrain suture
0.8
0.7
0.6
0.5
0.3
0.4
0.5
0.6
Position of fronto-parietal suture

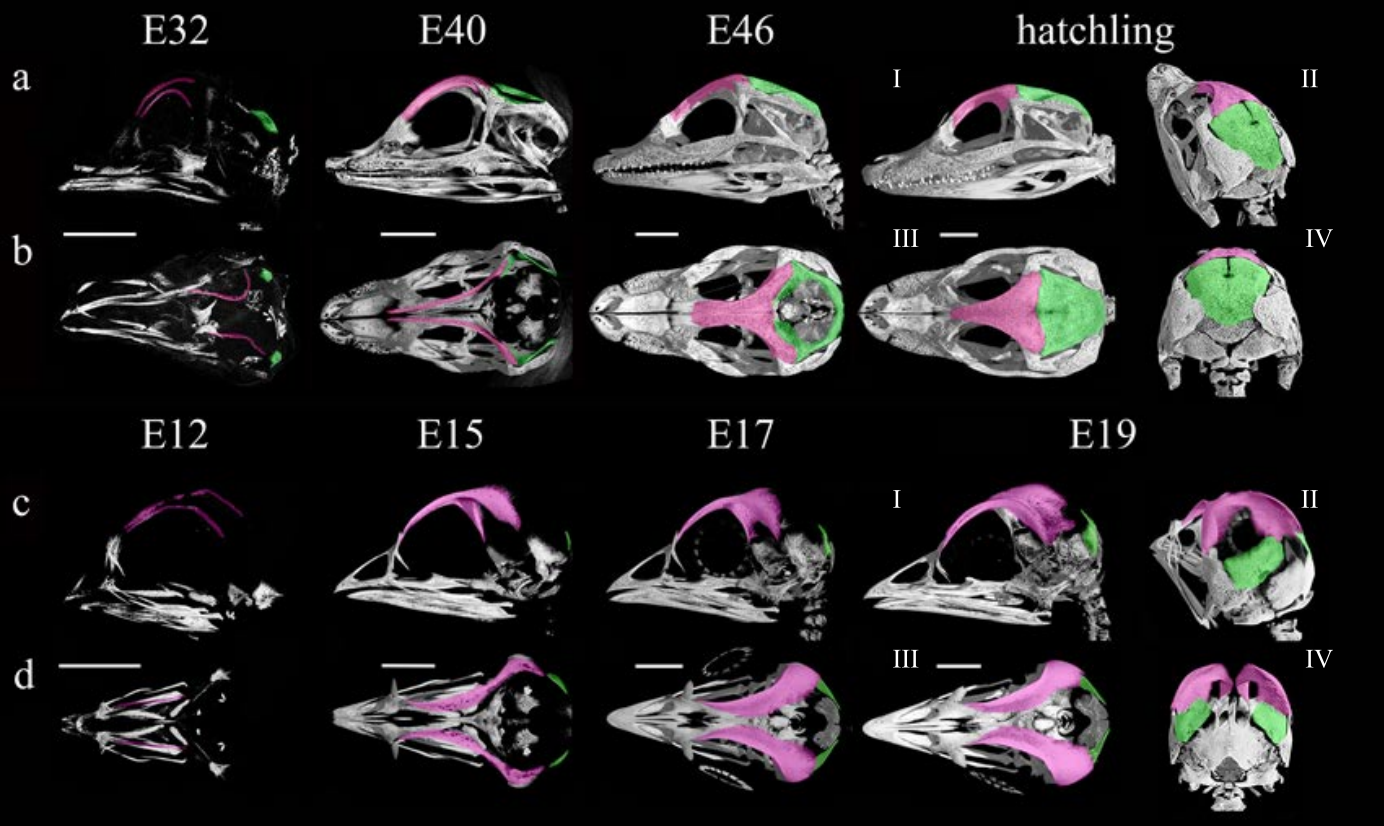
E32
E40
E46
hatchling
a
b
I
II
III
IV
E12
E15
E17
E19
c
d
I
II
III
IV

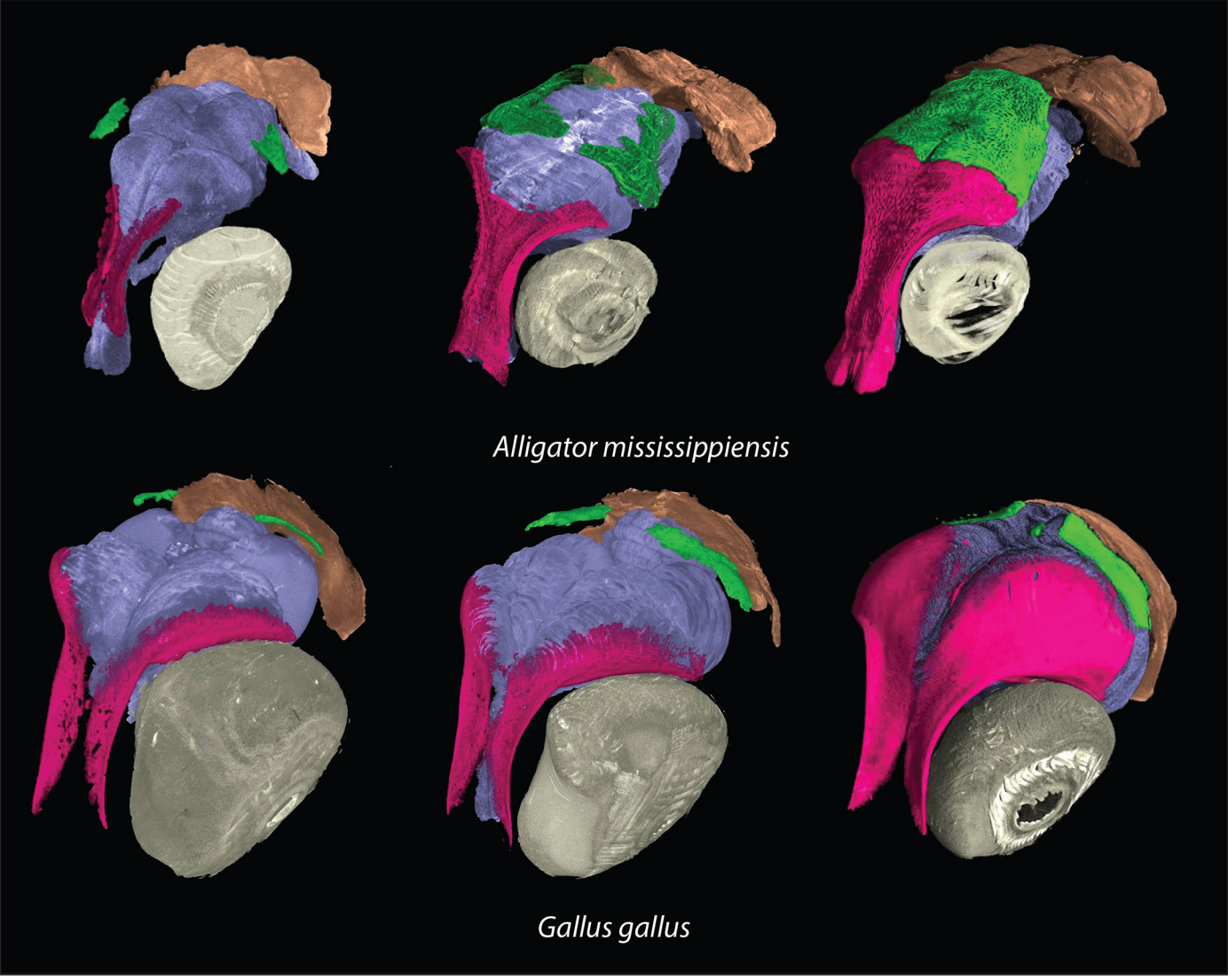

Alligator mississippiensis

Gallus gallus

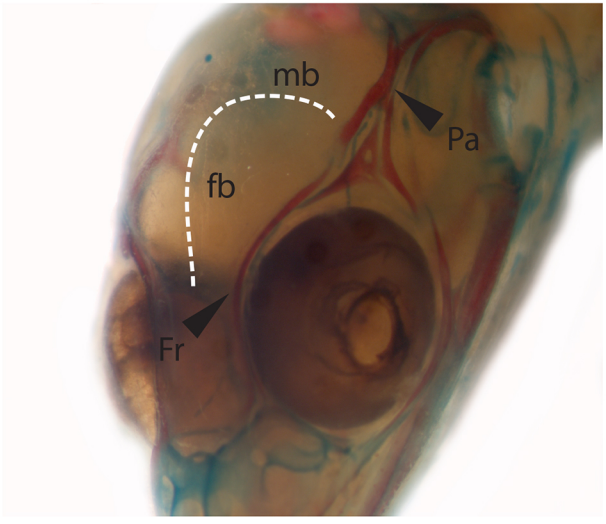

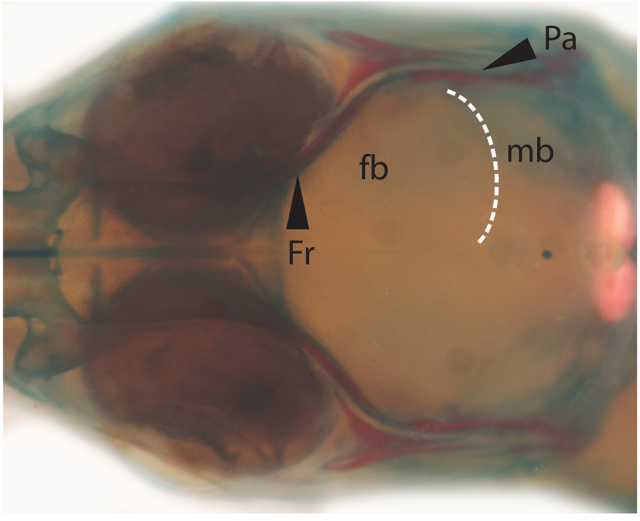

Chalcides chalcides